ORIGINAL PAPER

Research on the viscous flow transition of styrene-isoprene-styrene triblock copolymer by Rheology

Hengyu Luo[1] · Hui Han[1] · Houfang Chi[1] · Junyu Li[2] · Songmei Zhao[2] · Yong Tao[1] · Haiqing Hu[1,3]

Abstract
The viscous flow transition of triblock copolymer styrene-isoprene-styrene (SIS5562) was studied by rheological methods. A broad loss factor (tan δ) peak at 152.5 ℃ appeared on the dynamic viscoelastic spectrum under experimental conditions. Some similar peaks had been attributed to order-order transition (OOT) or order-disorder transition (ODT) in some research. In this system, the SAXS, time-temperature superposition (TTS) and Han plots proved that the microstructure of the SIS5562 did not undergo OOT or ODT transition in the temperature range. It may be the viscous flow transition as we supposed previously. The rheology study by capillary and rotation rheometer verified that the viscous flow transition temperature (T_f) was around 150 ℃.

Keywords Viscous flow transition · Rheology · SAXS · SIS

Introduction

Block copolymer refers to the copolymer formed by two or more block chains with different chemical properties connected together in different ways [1, 2]. Thermoplastic elastomer is a special block copolymer which combined the high elasticity of rubber at room temperature and the plasticity of plastic at high temperature [3]. They can be processed on traditional plastic equipment, such as injection molding, blow molding and profile extruders, etc [4, 5]. Thermoplastic elastomer exhibits a great industrial application value. Due to the thermodynamic incompatibility between different

blocks, complex microscopic phase separation exists in the inner structure of block copolymers [6, 7]. Many particular properties can exhibit, such as microphase separation structure [8, 9], order-order transition (OOT) [10], order-disorder transition (ODT) [11, 12], complex thermal rheology, etc. Microscopic phase separation and transition:the OOT and ODT had been carried out on star block copolymers [13], salt-doped deblock copolymers [14], linear triblock copolymers [15, 16], cross-linked block copolymers [17], graft block copolymers [18], copolymer/homopolymer blends [19] etc.

Linear A-B-A type thermoplastic elastomers are composed of a long elastomeric B block with low T_g and two relatively short thermoplastic blocks with high T_g. The presence of two T_g indicates that there is a microscopic phase separation between component A and B [20]. This special structure leads to the self-assembly of different blocks into a microphase structure from lamellar to hexagonally-stacked cylindrical and finally to spherical microdomains of cubic lattice [21]. Ivy Mathew et al. [22] investigated the viscous and elastic behavior of the saturated triblock copolymer polystyrene-block-poly (ethylene-co-butylene) -polystyrene (SEBS) through a capillary viscometer. The flow curve of SEBS showed obvious two-section straight line characteristics, which was due to the microphase separation leading to two different flow behaviors. Styrene and isoprene as monomer, triblock copolymers polystyrene-block-polyisoprene-block-polystyrene (SIS) were

✉ Junyu Li
  lijy@iccas.ac.cn

✉ Haiqing Hu
  hhq@qust.edu.cn

[1] Key Laboratory of Rubber-Plastics, Ministry of Education/ Shandong Provincial Key Laboratory of Rubber-plastics, School of Polymer Science and Engineering, Qingdao University of Science and Technology, Qingdao 266042, China

[2] CAS Key Laboratory of Engineering Plastics, Beijing National Laboratory for Molecular Sciences, Institute of Chemistry, Chinese Academy of Sciences, Beijing 100190, China

[3] State Key Laboratory of Polymer Materials Engineering, Sichuan University, Chengdu 610041, China

successfully synthesized by anionic polymerization using a difunctional t-BuLi initiator [23]. SIS is an excellent thermoplastic elastomer, which has been widely studied due to its complex structure. Naoki Sakamoto et al. [24] investigated the OOT and ODT of SIS in a solution dioctyl phthalate via SAXS and rheology. OOT took place at 130 ℃ ~ 140 ℃ and ODT at about 205 ℃. Chang Dae Han et al. [25] synthesized three SIS block copolymers with spherical, cylindrical and lamellar structures respectively. They observed that the morphological state of microdomain structure in the SIS block copolymers had a pronounced effect on the OOT. The Han curve was drawn to analyze the ODT of three SIS samples, which occurred at 180 ℃, 90 ℃ and 105 ℃, respectively. Naoki Sakamoto et al. [26] investigated OOT and ODT of a SIS copolymer by SAXS, TEM and rheological study. These results showed that the SIS formed hexagonally-packed cylindrical and spherical microdomains. Dino Ferri et al. [27] investigated the steady rheological behavior and the temperature dependence of phase behavior of three SIS with different M_w (molecular weight), narrow molecular weight distribution, and different PS (polystyrene) contents. The loss tangent obtained from the DMA showed that the three SIS all had a significant peak at about -53 ℃ and 100 ℃, corresponding to the glass transition (T_g) of the PI block and PS block. A distinct broad peak was observed around the temperature greater than 100 ℃. It was assigned to OOT or ODT depending on the weight content of PS in the compositions.

When studying the wall slip phenomenon of SIS (SIS1209), Hui Han et al. [28] found an unknown rheological response peak near 168.6 ℃ on the dynamic viscoelastic spectrum. The SAXS showed that there was no OOT or ODT at this temperature. It was proposed to be a viscous flow transition peak. In order to fully study this transition, another SIS5562 was investigated systematically. The molecular structure of SIS1209 and SIS5562 were listed in Table 1. More rheology analysis was introduced to explain this phenomenon, besides the DMA and SAXS in reference 28. The results verified the viscous flow theory further.

Experimental section

Materials

The linear SIS5562 was supplied by LCY Chemical COR Company (TaiWan, China). The linear SIS1209 was supplied by Baling Petrochemical Company (Hunan, China). The detailed molecular structure information of SIS5562 and SIS1209 were shown in Table 1.

Sample preparation

SIS particles were dried at 60 ℃ for 12 h in a vacuum drying oven. The dried SIS particles were hot-pressed, at a temperature of 150 ℃ and lasted for 15 minutes. Some SIS were tailored into disk specimens (the diameter was 25 mm and the thickness was about 1.5 mm) for the parallel plate tests. Some SIS were cut into rectangle (the length, width and thickness were 10.5 mm, 3.8 mm and 1.9 mm respectively) specimens for the torsion fixture tests.

Experimental characterization

Rheological measurement

The steady-state rheological properties of SIS were measured on RH2000 a constant-velocity double tube capillary rheometer. The diameter of the two barrels was 15 mm. The length-to-diameter ratio of the zero-length capillary (used to measure the entrance pressure drop) was 0.25/1 (mm/mm). The length-to-diameter ratio of the other normal capillary was 16/1 (mm/mm). The apparent shear rate varied from 20 s^{-1} to 2500 s^{-1}. The characterization temperature was from 140 ℃ to 200 ℃.

The dynamic mechanical properties of SIS were performed by Advanced Rheological Expansion System (ARES-G2, TA). There were two kinds of test modes:

1. Dynamic frequency sweep: Dynamic frequency sweep experiments were performed from 5×10^{-3} Hz to 100 Hz at different temperatures (130 ℃ ~ 200 ℃) with the parallel plate fixture test mode. All the experimental specimens were tested within the linear viscoelastic range. The experiment test adopted the sweep method from high frequency to low frequency.
2. Dynamic temperature sweep: Torsion fixture test mode were carried out at low temperature (-130 ℃ ~ 100 ℃, rectangle specimens). Parallel plate fixture test mode at high temperature (100 ℃ ~ 220 ℃, disk specimens) under nitrogen atmosphere. The temperature raising rate was 1.5 ℃/min, the strain was 1%, and the angular frequency was 1 Hz.

Table 1 Molecular characteristics of SIS1209 and SIS5562

Specimen	M_w / (g/mol)	M_w/M_n	S/I	M_w (PS) / (g/mol)	M_w (PI) / (g/mol)
SIS1209	1.22×10^5	1.1	29/71	1.77×10^4	8.67×10^4
SIS5562	8.30×10^4	1.1	45/55	1.87×10^4	4.57×10^4

Small-angle X-ray scattering (SAXS)

The SAXS experiments were conducted using a GANE-SHA 300XL+ system. The instrument was equipped with a Pilatus 300K detector with pixel size of 172 μm × 172 μm. The wavelength was 1.54 Å. The detector was kept in a vacuum chamber. The distance between the specimen and the detector varied between 0.115 m and 1.47 m, depending on the configuration used. Silver behenate was used as the calibration standard. The range of q varied from 0.003 to 3 $Å^{-1}$. The specimen was first placed between Aluminum foils with temperature control using a temperature stage (Linkam. U.K.). The vacuum chamber was evacuated before temperature increase. Then the temperature was firstly increased from room temperature (25 ℃) to 200 ℃ at a rate of 10 ℃/min. The SAXS measurement was conducted during cooling at the same rate (10 ℃/min). After the specimen reached the set temperature (i.e. 200 ℃, 180 ℃, 160 ℃, 140 ℃, 120 ℃), it was equilibrated for 5 min before the measurement. The accumulation time was 30 min. In this paper, microstructure of SIS in the capillary extrusion process under various temperatures was studied. The time required for SIS melt to flow through the capillary is very short (less than 5 min). That is reason that the annealing time for SAXS measurement was selected as 5 min. The SAXS data was processed via SAXSGUI program.

Transmission electron microscope (TEM)

The structure of microphase separation was observed by transmission electron microscope (TEM, JEM-2100). Because the electron density contrasts were small, the SIS needed to be dyed before measurement. Firstly, the SIS sample was immersed and stained in an aqueous solution of osmium tetroxide ($w = 4$ wt%) for 20 min. Then ultra-thin sectioning was performed at a temperature below T_g.

Results and discussion

Temperature scan spectrum of SIS

Figure 1 showed the curve of the dynamic mechanical loss factor by temperature scanning of SIS5562. It could be seen in Fig. 1 that SIS5562 had three rheological response peaks. The peak around -47 ℃ corresponded to the glass transition temperature of the soft PI block ($T_{g, PI}$) in the SIS system. The peak around 100 ℃ corresponded to the glass transition temperature of the hard PS block ($T_{g, PS}$). The existence of two obvious glass transition peaks demonstrated that PS and PI blocks had microscopic phase separation [29]. The third obvious rheological response peak was at around 152.5 ℃. Compared to the $T_{g, PI}$ or $T_{g, PS}$, this peak was much broader.
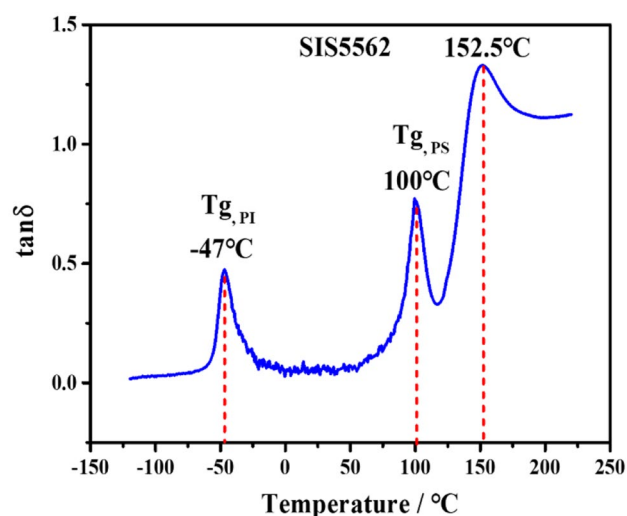

Fig. 1 Temperature dependence of dynamic-mechanical loss factor of SIS5562

Obviously, it was not the glass transition peak. Many literatures had reported the similar rheological response peaks. Hashimoto T. et al. [26] attributed it to the loss peak caused by the transformation of SIS melt from one ordered structure to another, OOT. The SAXS showed the transition from one order to another. Canetti M. et al. [27] assigned it to the ODT because they found that the abrupt drop of G' was taken as a signature of the complete mixing of the PS and PI blocks. In the previous paper [28], we proposed that it was a viscous flow transition, because the SAXS showed the structure did no change. We would discuss systematically about this transition in the following sections through rheology and other analysis. First, the micro structure was investigated through TEM and SAXS.

Microstructure characterization of SIS5562

Because of thermodynamic incompatibility, the PS blocks and the PI blocks in SIS would undergo microphase separation [28]. The microstructure of SIS5562 at room temperature was shown in Fig. 2a. The dark (black) areas represented the PI microdomains stained by osmium tetroxide. The light (white) areas represented the PS microdomains, which was not stained. The dark areas and the light areas were distributed alternately, showing a regular lamellar micro structure.

The SAXS profiles of SIS5562 obtained at different temperature during cooling was given in Fig. 2b. The curves under a series of temperatures had been moved vertically to make the results more clearly. The SAXS profiles of SIS5562 showed multiple interparticle scattering peaks caused by the long-range order periodic microdomain structure. According to the ratio of each scattering vector q of the corresponding scattering peak, the relative positional relationship of the
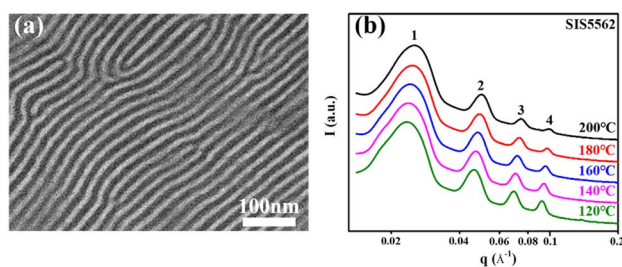
Fig. 2 TEM photomicrograph at room temperature (**a**) and SAXS profiles during cooling at different temperatures (**b**)

four scattering peaks was 1:2:3:4, no matter the test temperature. It indicated that the microphase structure of SIS5562 did not change. The lamellar microdomain phase structure invariably maintained within the range of test temperature (120 ℃ ~ 200 ℃), indicated that the SIS5562 had good regularity and uniformity. The scattering intensity gradually enhanced with the decrease of the temperature, implied that the microphase separation became coarser with the decrease of temperature. In summary, during the temperature range of 120 ℃ to 200 ℃, SIS5562 had always maintained lamellar structure. There was no OOT or ODT within the test temperature range (i.e. 120 ℃ ~ 200 ℃).

Generally, the rheological properties were related to the structure of polymer melts. Therefore, the following rheology analysis was carried out to verify this result further.

Time-temperature superposition of SIS5562

The time-temperature superposition (TTS) principle was first proposed by Williams et al. [30, 31]. The TTS theory could be applied in experiments investigating time and frequency dependency of materials' behavior to predict their long-term viscoelastic properties [32]. TTS asserted that for a thermal rheological simple material, a change in temperature would have the same effect on the viscoelastic properties as a corresponding change in time. It could be used to define the relationship between time and temperature based on the deformation and relaxation response of a viscoelastic material under constant stress or strain conditions [33–35]. In other words, the TTS implies that time or frequency is equivalent to temperature [36]. The data obtained from the tests were manipulated to produce rheological master curves [31, 37]. The modulus measured at different temperatures could be shifted horizontally and vertically with shift factors α_T and b_T, respectively [38]. The TTS principle function is [38–41]:

$$G^{'}\left(\omega, T_{ref}\right) = b_T \cdot G^{'}\left(\alpha_T \cdot \omega, T\right) \tag{1}$$

where $G^{'}$ is the storage modulus; ω is the frequency; α_T and b_T are horizontal and vertical shift factors, respectively; T_{ref} is the reference temperature. The vertical shift factor b_T should, generally, be small [42]. b_T results the relationship between temperature and modulus, is defined as [42, 43]:

$$b_T = \frac{G^{\infty}\left(T_{ref}\right)}{G^{\infty}(T)} \tag{2}$$

where G^{∞} is the plateau value of $G^{'}$ (at high frequencies). G^{∞} is proportional to $k_B \cdot T$ for a purely entropic network and it is also proportional to the number density of active elastic chains. k_B is the Boltzmann factor [42].

The horizontal shift factor α_T represents the relationship between temperature and frequency (relaxation time) [43], defined as [44]:

$$\alpha_T = \frac{\tau_T}{\tau_{ref}} \tag{3}$$

where τ_{ref} is the relaxation time at T_{ref}, and τ_T is the time required to give the same response at the test temperature T.

Some study [45, 46] of TTS master curve of dynamic storage modulus of block copolymers explored that the character of TTS in low frequency region could be used to explain the microphase structure of block copolymers. This is because that the viscoelastic response in the low frequency region reflects the relaxation behavior of the nano-scale micro-domain structure. Once the OOT or ODT happened for block copolymers, their microphase structures will change. The TTS curve would be much complex than the curve of a homopolymer without the structure change [47, 48].

Due to the complex rheological behavior of SIS, horizontal and vertical shifts were performed via TRIOS software (the software from the TA). The data of the storage modulus at different temperatures on the TTS master curve was shown in Fig. 3. Since the special rheological response peak appeared near 150 ℃ in Fig. 1, 150 ℃ and 160 ℃ were selected as the reference temperature. Table 2 provided detailed information about α_T and b_T at each temperature.
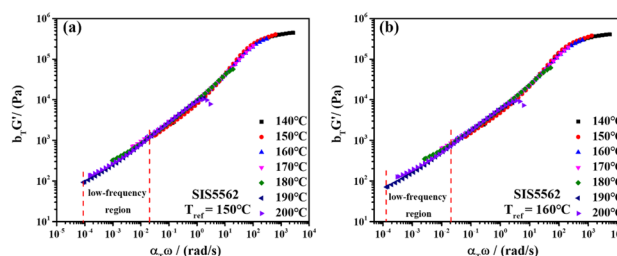
Fig. 3 TTS master curve of SIS5562 at different temperatures (**a**) T_{ref} = 150 ℃ (**b**) T_{ref} = 160 ℃

In Fig. 3a, 150 ℃ was taken as the reference temperature, the TTS master curve was almost smooth in the whole frequency range without significant temperature dependence. Especially, there was no obvious temperature dependence in the low-frequency region ($8 \times 10^{-5} \sim 0.02$ rad/s). It indicated that the microstructure of SIS5562 hardly changed within the experimental temperature range [46]. When 160 ℃ was taken as the reference temperature, as shown in Fig. 3b, there was also no significant temperature dependence across the experimental range. The master curve was nearly smooth, which further proved that the microstructure of SIS5562 did not change in the experimental temperature range. In this case, the TTS results supported that there was no OOT or ODT occurred around 150 ℃, which was consistent with the SAXS results.

log *G′* vs log *G″* (Han plots)

The Han plot [25, 49–51] was originally proposed for homogeneous system. It was believed that the order-disorder transition of materials could be determined through the temperature dependence of rheology. According to the common stress relaxation phenomenon of viscoelastic materials, the stress-strain response of the materials in the linear viscoelastic region satisfied the Blotzmann superposition principle. Han curve was the relation curve of log $G'(\omega)$ vs log $G''(\omega)$ deriving from the modulus data. The relationship was obtained through the following function [52, 53]:

$$lgG' = x \cdot lgG'' + (1-x) \cdot lg\left(8G_N^0/\pi^2\right) \tag{4}$$

where, $1<x<2$, is the slope of log Han plot. It is less than 2 for polydisperse polymers in the terminal region [52]. G_N^0 is the plateau modulus [52, 54].

Figure 4 was log $G'(\omega)$ versus log $G''(\omega)$ plots drawn based on frequency sweep data at different temperature, which was manipulated from data in Fig. 8. When studying the OOT of the triblock copolymer SIS (Vector 4111), Naoki Sakamoto et al. [26] firstly observed that a negative slope in the sharp change in Han plots in the terminal region at temperatures ranging from 185 ℃ to 210 ℃. The threshold temperature was ca.185 ℃, which corresponded to the onset of OOT [26]. The negative slope disappeared when the temperature was above 210 ℃, which was the end of the OOT
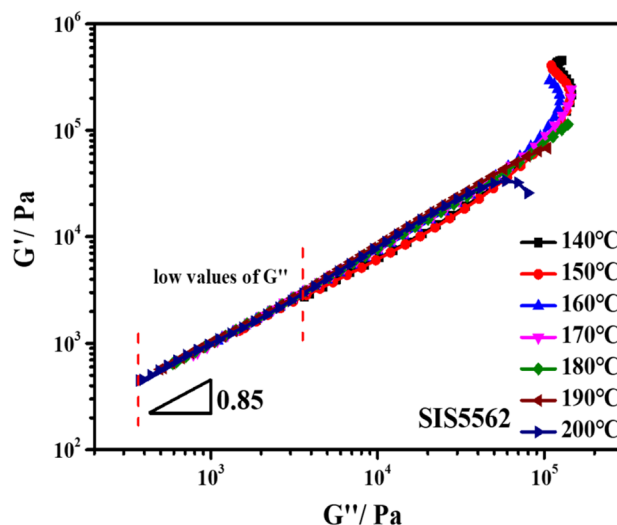

Fig. 4 Han plots of SIS5562 at different temperatures

transition [26]. Therefore, the negative slop represented the OOT transition in the system. In Fig. 4, the Han curve of SIS5562 did not show any negative slope at the terminal region (low values of G'') in the whole range of experimental temperature. It indicated that no OOT occurred during the experimental test.

When studying the ODT of block copolymers, Han C. D. et al. [51] found that Han plots for an SIS block copolymer varied gradually with the increasing of temperature up to a certain critical value. Then it became virtually independent of temperature as the temperature increased further. When determining the ODT temperature of SIS, Kim J. et al. [50] found that the Han curve for the SIS block copolymer exhibited strong temperature dependence, especially at low values of G''. It was attributed to the transition from an ordered microdomain structure to a disordered homogeneous phase (ODT). If ODT did not occurred in SIS melt within the experimental temperature range, the Han plots was temperature independent. In Fig. 4, the Han plots had virtually no temperature dependence in the terminal region (low values of G'', 367.2 ~ 3550.6 Pa), indicated that no ODT occurred. The terminal slopes (around 0.85) of the Han plots (Fig. 4) of SIS5562 were much less than 2, indicated that SIS5562 maintained microphase separation in the whole test process. There was no ODT below

Table 2 Details of α_T and b_T at different temperatures ($T_{ref} =$ 150 ℃ and 160 ℃)

|	T/℃	140	150	160	170	180	190	200
$T_{ref} = 150$ ℃	α_T	4.22	1.00	0.48	0.16	0.03	2.85×10^{-3}	4.74×10^{-3}
	b_T	0.98	1.00	1.07	0.89	0.49	0.16	0.31
$T_{ref} = 160$ ℃	α_T	8.56	2.07	1.00	0.33	0.08	4.21×10^{-3}	9.86×10^{-3}
	b_T	0.89	0.93	1.00	0.81	0.54	0.13	0.28

200 °C. In summary, the TTS and Han plot implied that SIS5562 did not undergo OOT or ODT within the experimental temperature range.

Temperature dependence of *G'* and *G''*

The microstructure of a material determines its macroscopic properties. Subtle change in the microstructure could be reflected in abrupt changes in its macroscopic properties, such as the modulus of the material. The dynamic mechanical measurements (DMA) was used to characterize the viscoelastic transition of polymer [28].

Figure 5a, b showed the storage modulus (G') and the loss modulus (G'') of the SIS5562 versus temperature. It could be seen that, within the measured temperature range, G' and G'' all gradually decreased with the increase of temperature. However, the slopes of the G' curve changed (from -0.039 to -0.013) at around 157.1 °C as shown by the red dotted line in the Fig. 5a. The temperature (157.1 °C) in the intersection point was defined as the critical temperature. This was very close to the temperatures of 152.5 °C in Fig. 1, which corresponded to the rheological response peak. Stephan Forster et al. [47] proposed that the OOT and the ODT between the ordered structures of polymers could be determined by the change of storage modulus with temperature. In literature 47, a discontinuous decrease of the storage modulus was attributed to be an ODT. The storage modulus increases considerably within a narrow temperature range indicated that the system undergone a phase transition between two ordered states, that was, OOT. This was an obviously different trend from the curve in Fig. 5a. In Fig. 5a, there was no discontinuous decrease but a turning point. Therefore, SIS5562 did not experience OOT or ODT within the test temperature range. This conclusion was in consistent with the previous analysis results of SAXS, TTS principle and Han plots.

As mentioned in reference 28, this transition was probably a viscous flow transition of the whole polymer chain. The temperature was the viscous flow transition temperature (T_f) [28]. When the viscous flow transition occurred, the polymer underwent a transition from a high elastic state to
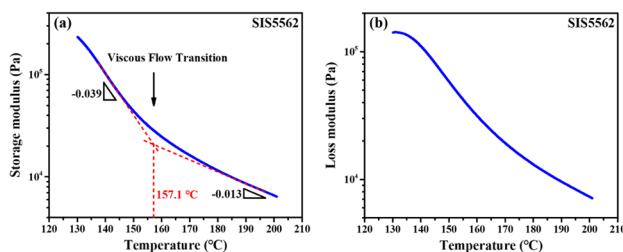
a viscous flow state [55]. A polymer material in the viscoelastic region may at times be considered as either elastic or viscous, or both [55]. In the SIS system, there were two block parts. The soft PI chains turned into the viscous flow state when temperature was much lower the T_f (around 150 °C). While PS part kept in elastic state below T_f. The PS phase in SIS melts experienced the change from the high elastic state to the viscous flow state [56] before and after the critical temperature T_f. When the temperature was lower than T_f, the storage modulus of the SIS5562 system was mainly contributed by the PS elastic phase. Because at this temperature the PI phase was in the state of viscous flow, the G'_{PI} was quite lower; PS phase was in the state of high elastic, the G'_{PS} was relatively higher. When the temperature was higher than T_f, the whole polymer chain turned into the viscous flow state with the viscous flow transition of PS microdomain. As a result, the G' decreased quickly, and the decrease rate of G' slowed down. The viscous flow transition for the block polymer was different for that of a homopolymer [28]. According to literature 28, the T_f of SIS1209 was about 170 °C, while T_f of SIS5562 was about 150 °C. This was because the molecular weight of SIS1209 (1.22×10^5 g/mol) was much higher than SIS5562 (8.30×10^4 g/mol), as showed in Table 1. T_f represents the temperature at which the entire polymer chains begin to move freely. Therefore, for the SIS system, when the temperature is lower than T_f, the PS phase region is under the state of high elastic. When temperature is higher than T_f, the PS phase region goes into the viscous flow state. As a result, the whole SIS molecular chain move freely. The larger the molecular weight of polymer chains, the higher the viscous flow temperature (T_f). Although the molecular weight of PS block in SIS5562 (M_w(PS)=1.87×10^4 g/mol) is slightly greater than that in SIS1209 (M_w(PS)=1.77×10^4 g/mol), the molecular weight of SIS1209 (1.22×10^5 g/mol) is much greater than SIS5562 (8.30×10^4 g/mol), so the T_f of SIS1209 is higher.

The flow behavior

Figure 6 shows the flow curves of SIS5562 at different temperatures. When the temperature was relatively low (140 °C ~ 160 °C), there were obvious turning points in the flow curve (A, B, and C in Fig. 6). The shear stress and the shear rate corresponding to the turning point was noted as critical shear stress (σ_c) and critical shear rate ($\dot{\gamma}_c$), respectively. With the increase of temperature from 140 °C to 160 °C, the critical shear rate corresponding to the turning point increased gradually from 165.4 s^{-1} to 1142.9 s^{-1}; while the critical shear stress decreased gradually from 372.3 kPa to 331.2 kPa. The critical shear rate and critical shear stress at different temperatures were detailed in Table 3.
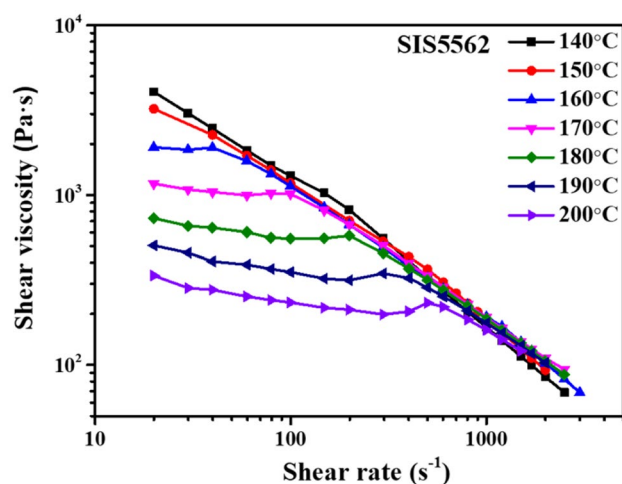
The shear stress increased sharply with the increased of the shear rate before the turning point. While after the

Fig. 5 Temperature dependence of G' (**a**) and G'' (**b**) of SIS5562 (f = 1Hz)
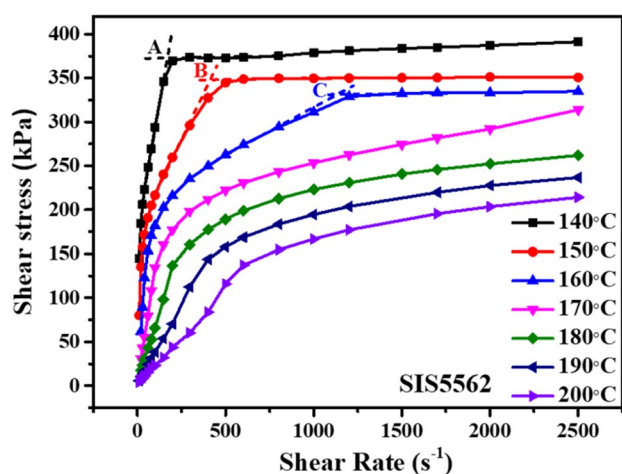
Fig. 6 The flow curve of SIS5562 at different temperatures

Fig. 7 Temperature dependence of the shear viscosity for SIS5562

turning point, the shear stress changed slightly with the increased of the shear rate or even kept constant. After the temperature exceeded 160 ℃, the turning point disappeared. This phenomenon could be explained from the viscous flow transition point of view. When the temperature was below the T_f (140 ℃ ~ 160 ℃), the PS phase was in the state of high elastic, the PS microdomain maintained. It played a role of physical crosslinking point (PS microdomain) in the SIS melt [28]. The SIS melt was considered to be a strong entangled system. Under the low shear rate (less than the critical shear rate), the shear stress was not big enough to destroy the physical crosslinking point (PS microdomain), the PS microdomain maintained. The shear stress increased much with the increase of shear strain. When the shear rate was greater than the critical shear rate, the physical crosslinking of the PS phase was destroyed under strong shear action. The flow was much easier, the shear stress almost kept the same level when the shear rate increased. Therefore, the flow curve showed a clear turning point. When the SIS flowed in a temperature higher than the T_f (170 ℃ ~ 200 ℃), well, the whole polymer chain was in the state of viscous flow state. Very low shear stress would destroy the microphase structure of the SIS. There were no microdomains as the crosslinking point in the system. The SIS melt transformed into a weaker entangled system [28]. The SIS flowed just like the normal homopolymers. No turning point appeared in the flow curve.

Figure 7 was the variation curves of shear viscosity with shear rate of SIS5562 at different temperatures. SIS5562

exhibited shear-thinning behaviors [57] at all temperatures. It was obviously that at relatively low shear rates, the shear viscosity varied greatly at high and low temperature. The viscosity curve of SIS5562 exhibited the "First Newtonian or Primary Newtonian plateau" [57, 58] when the temperature was in the range of 160 ℃ ~ 200 ℃. As we know, for pseudoplastic fluids, when the shear rate tends to zero, the fluid viscosity tends to be constant, which is called the first Newtonian plateau. The viscosity is called the zero-shear viscosity. This is the reflection of high viscous properties. The corresponding shear rate range of the "First Newtonian plateau" expanded with the increase of temperature, showed in Table 4.

When the temperature was lower than 160 ℃, the "First Newtonian plateau" did not exist in the viscosity curve at low shear rates. This peculiar phenomenon could be related to the viscous flow transition of PS microphase in SIS melt. When the temperature was below 160 ℃, the PS microdomain existed in the SIS melt in the high elastic state, acting as a physical cross/linking point. The system showed a strong elastic behavior, with less viscous behavior. The "First Newtonian plateau" did not appear on the viscosity curve, because it was the reflection of viscous behavior. When the temperature was higher than 160 ℃, the PS microdomains in the SIS melt changed from a highly elastic state to a viscous flow state. The entire SIS molecular chain completely entered a viscous flow state. In this case, the entanglement between the molecular chains weakened much. The elasticity receded and the viscous property enhanced. The flow of SIS

Table 3 Critical shear stresses and critical shear rates of SIS5562 at different temperatures	Temperature/℃	140	150	160	170	180	190	200
	$\dot{\gamma}_c$/(s⁻¹)	165.4	413.9	1142.9	---	---	---	---
	σ_c/(kPa)	372.3	347.7	331.2	---	---	---	---

Table 4 Shear rate range of the "First Newtonian plateau" at different temperatures

| T/℃	160	170	180	190	200
Range/ s⁻¹	20 ~ 41	20 ~ 102	20 ~ 200	20 ~ 307	20 ~ 525

was just similar to the homopolymer. The "First Newtonian plateau" appeared on the viscosity curve. The higher the temperature is, the broader the "First Newtonian plateau".

Dynamic rheological measurements

Small amplitude oscillation shear methods are usually used in the dynamic rheological test of polymer materials. The testing process will not damage or affect the structure of the polymer materials under the low shear rate and stress. Moreover, the dynamic rheological parameters of polymer materials in the linear viscoelastic region are very sensitive

Fig. 8 Dynamic storage modulus G' (**a**) and loss modulus G'' (**b**) of SIS5562 as a function of ω at different temperatures

to the morphology and structure. Therefore, dynamic rheological methods can effectively characterize the structural changes of polymer materials [59–61]. Figure 8 were the plots of the dynamic storage modulus (G') and loss modulus (G'') of SIS5562 as a function of angular frequency (ω) at different temperatures (140 ℃ ~ 200 ℃). In the Fig. 8a, with the increase of temperature, the G' of the SIS5562 decreased gradually throughout the test range. It meant that the thermal motion ability of the molecular chain increased gradually and the elasticity of the polymer melt decreased gradually. What's more, within the test range, the series of log G' vs log ω curves could be divided into two groups by 150 ℃. Below 150 ℃ (that was 140 ℃), the G' within the test frequency range was significantly higher than that at other temperatures (150 ℃ ~ 200 ℃). This can be attributed to the fact that PS phase in the SIS melt was in the state of elasticity with high modulus. It gradually entered into viscous flow state above T_f (150 ℃) with low modulus. The entire SIS molecular chain started to move freely, so G' significantly decreased at the same angular frequency.

Figure 8b given plots of log G'' vs. log ω for SIS5562. It could be seen that the log G'' vs log ω curves could also be divided into two groups by 150 ℃. It was the same reason as discussed above. These peculiar phenomena can be attributed to viscous flow transition of PS microphase in SIS melt. In other words, when the experimental temperature was below T_f, strong entanglement was formed between SIS molecular chains due to the existence of the PS microdomains. The strong entanglement required a greater external stress to destroy. When the experimental temperature was higher than T_f, the PS chains entered a viscous flow state. The PS microdomains was easy to be damaged under the flow stress. The entanglement only formed among SIS molecular chains which could be disentangled under relatively low external force. Therefore, compared with G' and G'' at low temperature (140 ℃), G' and G'' at high temperature (150 ℃ ~ 200 ℃) were significantly lower at the same angular frequency, especially at the terminal region of low frequency.
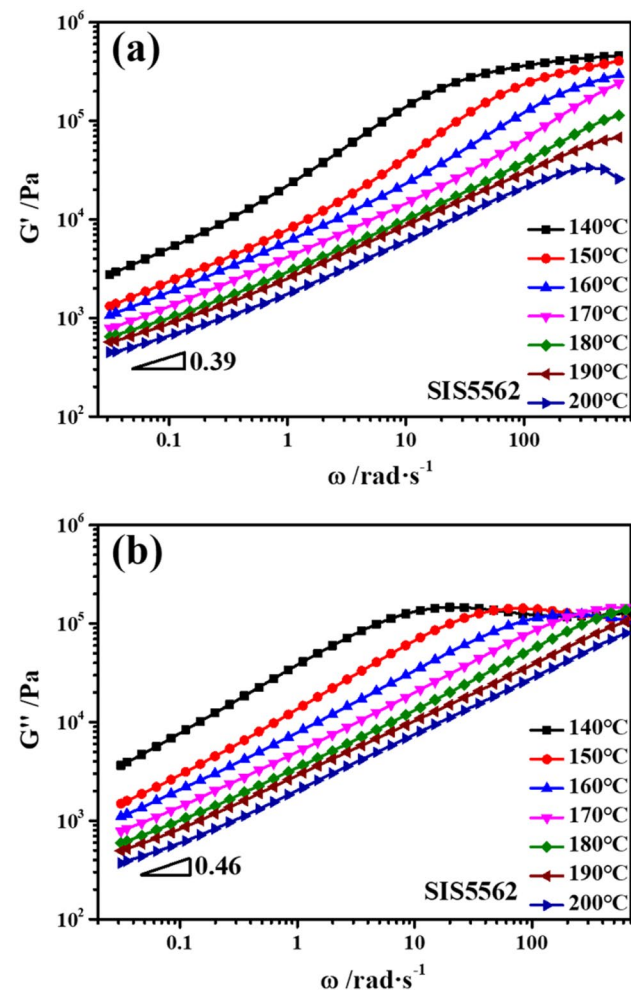
Conclusion

A broad peak at 152.5 ℃ was shown in the DMA viscoelastic curve of SIS5562. The SAXS, TTS and Han plots demonstrated that this thermodynamic transitions of SIS5562 at/near 152.5 ℃ was not OOT or ODT. It was supposed that this was the viscous flow transition temperature of PS microphase in SIS melt. From this point of view, the viscous flow transition of SIS was systematically investigated through the rheological methods. Based on this viscous flow transition and structure characterization, the special flow behavior under both static and dynamic

state could be explained reasonably. It confirmed that the viscous flow transition temperature of SIS5562 was around 150 ℃.

Reference

1. Bates FS, Fredrickson GH (1999) Block copolymers—designer soft materials. Phys Today 52:32–38
2. Bates FS, Hillmyer MA, Lodge TP, Bates CM, Delaney KT, Fredrickson GH (2012) Multiblock polymers: panacea or pandora's box? Science 336:434–440
3. Yang HW, Canich JAM, Licciardi GF (1996) Thermoplastic elastomers. US
4. Bonart R (1979) Thermoplastic elastomers. Polymer 20:1389–1403
5. Holden G, Bishop ET, Legge NR (2010) Thermoplastic elastomers. Journal of Polymer Ence Part C Polymer Symposia 26:37–57
6. Bates FS, Fredrickson GH (1990) Block copolymer thermodynamics: theory and experiment. Annu Rev Phys Chem 41:525–557
7. Lee H-K, Zin W-C (2000) Phase diagrams for the blends of a styrene-butadiene diblock copolymer and a styrene-butadiene random copolymer: Theory. Macromolecules 33:2894–2900
8. Zhu Y, Gido S, Iatrou H, Nikos H, Mays J (2003) Microphase separation of cyclic block copolymers of styrene and butadiene and of their corresponding linear triblock copolymers. Macromolecules 36:148–152
9. Yamaguchi D, Hashimoto T, Han CD, Baek DM, Kim JK, Shi A-C (1997) Order−disorder transition, microdomain structure, and phase behavior in binary mixtures of low molecular weight polystyrene-block-polyisoprene copolymers. Macromolecules 30:5832–5842
10. Wanakule NS, Panday A, Mullin SA, Gann E, Hexemer A, Balsara NP (2009) Ionic conductivity of block copolymer electrolytes in the vicinity of order−disorder and order−order transitions. Macromolecules 42:5642–5651
11. Bates F, Rosedale J, Fredrickson G (1990) Fluctuation effects in a symmetric diblock copolymer near the order-disorder transition. J Chem Phys 92:6255–6270
12. Ogawa T, Sakamoto N, Hashimoto T, Han CD, Baek DM (1996) Effect of volume fraction on the order− disorder transition in low molecular weight polystyrene-block-polyisoprene copolymers. 2. Order− disorder transition temperature determined by small-angle X-ray scattering. Macromolecules 29:2113–2123
13. Hashimoto T, Ijichi Y, Fetters L (1988) Order–disorder transition of starblock copolymers. J Chem Phys 89:2463–2472
14. Qin J, de Pablo JJ (2016) Ordering transition in salt-doped diblock copolymers. Macromolecules 49:3630–3638
15. Winter HH, Scott DB, Gronski W, Okamoto S, Hashimoto T (1993) Ordering by flow near the disorder-order transition of a triblock copolymer styrene-isoprene-styrene. Macromolecules 26:7236–7244
16. Krishnamoorti R, Modi MA, Tse MF, Wang HC (2000) Pathway and kinetics of cylinder-to-sphere order−order transition in block copolymers. Macromolecules 33:3810–3817
17. Hahn H, Chakraborty AK, Das J, Pople JA, Balsara NP (2005) Order−disorder transitions in cross-linked block copolymer solids. Macromolecules 38:1277–1285
18. Maher MJ, Jones SD, Zografos A, Xu J, Schibur HJ, Bates FS (2018) The order-disorder transition in graft block copolymers. Macromolecules 51:232–241
19. Lee S-H, Char K, Kim G (2000) Order−disorder and order−order transitions in mixtures of highly asymmetric triblock copolymer and low molecular weight homopolymers. Macromolecules 33:7072–7083
20. Leibler L (1980) Theory of microphase separation in block copolymers. Macromolecules 13:1602–1617
21. Tanaka Y, Hasegawa H, Hashimoto T, Ribbe A, Sugiyama K, Hirao A, Nakahama S (1999) A study of three-phase structures in ABC triblock copolymers. Polym J 31:989–994
22. Mathew I, George KE, Francis DJ (1994) Viscous and elastic behaviour of SEBS triblock copolymer. Die Angewandte Makromolekulare Chemie 217:51–59
23. Lee P-C, Wang C-C, Chen C-Y (2020) Synthesis of high-vinyl isoprene and styrene triblock copolymers via anionic polymerization with difunctional t-BuLi initiator. Eur Polym J 124:109476
24. Sakamoto N, Hashimoto T, Han CD, Kim D, Vaidya NY (1997) Effect of addition of a neutral solvent on the order−order and order−disorder transitions in a polystyrene-block-polyisoprene-block-polystyrene copolymer. Macromolecules 30:5321–5330
25. Han CD, Baek DM, Kim JK (1990) Effect of microdomain structure on the order-disorder transition temperature of polystyrene-block-polyisoprene-block-polystyrene copolymers. Macromolecules 23:561–570
26. Sakamoto N, Hashimoto T, Han CD, Kim D, Vaidya NY (1997) Order−order and order−disorder transitions in a polystyrene-block-polyisoprene-block-polystyrene copolymer. Macromolecules 30:1621–1632
27. Ferri D, Canetti M (2006) Spurt and melt flow distorsions of linear styrene-isoprene-styrene triblock copolymers. J Rheol 50:611–624
28. Han H, Tian G, Gao Q, Hu H, Zhao J, Li J (2020) Wall slip of styrene-isoprene-styrene (SIS) triblock copolymer induced by micro elastic phase. Polymer 209:122990
29. Leibler Ludwik (1980) Theory of microphase separation in block copolymers. J Dalian Inst Tech 13:1602–1617
30. Williams ML, Landel RF, Ferry JD (1955) The temperature dependence of relaxation mechanisms in amorphous polymers and other glass-forming liquids. J Am Chem Soc 77:3701–3707
31. Wang M-J, Lu SX, Mahmud K (2000) Carbon–silica dual-phase filler, a new-generation reinforcing agent for rubber. Part VI. Time–temperature superposition of dynamic properties of carbon–silica-dual-phase-filler-filled vulcanizates. J Polym Sci B Polym Phys 38:1240–1249
32. Mahdavi R, Goodarzi V, Ali Khonakdar H, Hassan Jafari S, Reza Saeb M, Shojaei S (2018) Experimental analysis and prediction of viscoelastic creep properties of PP/EVA/LDH nanocomposites using master curves based on time–temperature superposition. J Appl Polym Sci 135:46725
33. Collins DA, Yakacki CM, Lightbody D, Patel RR, Frick CP (2016) Shape-memory behavior of high-strength amorphous thermoplastic poly(para-phenylene). J Appl Polym Sci 133:42903
34. Vaidyanathan TK, Vaidyanathan J, Cherian Z (2003) Extended creep behavior of dental composites using time–temperature superposition principle. Dent Mater 19:46–53
35. Zhang T, Zhao Y, Zhang B (2018) A method based on the time–temperature superposition principle to predict pressurization time in compression molding. J Appl Polym Sci 135:46664
36. Nakano T (2013) Applicability condition of time–temperature superposition principle (TTSP) to a multi-phase system. Mech Time-Depend Mater 17:439–447

37. Jamarani R, Erythropel HC, Burkat D, Nicell JA, Leask RL, Maric M (2017) Rheology of green plasticizer/poly(vinyl chloride) blends via time-temperature superposition. Processes 5:43

38. Vananroye A, Leen P, Van Puyvelde P, Clasen C (2011) TTS in LAOS: validation of time-temperature superposition under large amplitude oscillatory shear. Rheologica Acta 50:795–807

39. Dealy J, Plazek D (2009) Time-temperature superposition-a users guide. Rheol Bull 78:16–31

40. Naya S, Meneses A, Tarrío-Saavedra J, Artiaga R, López-Beceiro J, Gracia-Fernández C (2013) New method for estimating shift factors in time–temperature superposition models. J Therm Anal Calorim 113:453–460

41. Bae J-E, Cho KS, Seo KH, Kang D-G (2011) Application of geometric algorithm of time-temperature superposition to linear viscoelasticity of rubber compounds. Korea-Australia Rheology Journal 23:81–87

42. Chronakis IS, Doublier J-L, Piculell L (2000) Viscoelastic properties for kappa- and iota-carrageenan in aqueous NaI from the liquid-like to the solid-like behaviour. Int J Biol Macromol 28:1–14

43. Oroian M, Amariei S, Escriche I, Gutt G (2013) A viscoelastic model for honeys using the time-temperature superposition principle (TTSP). Food Bioprocess Technol 6:2251–2260

44. Tsuji T, Mochizuki K, Okada K, Hayashi Y, Obata Y, Takayama K, Onuki Y (2019) Time–temperature superposition principle for the kinetic analysis of destabilization of pharmaceutical emulsions. Int J Pharm 563:406–412

45. Kossuth MB, Morse DC, Bates FS (1999) Viscoelastic behavior of cubic phases in block copolymer melts. J Rheol 43:167–196

46. Hadjichristidis N, Pispas S, Floudas G (2003) Viscoelastic properties of block copolymers. John Wiley & Sons, Ltd

47. Foerster S, Khandpur AK, Zhao J, Bates FS, Hamley IW, Ryan AJ, Bras W (1994) Complex phase behavior of polyisoprene-polystyrene diblock copolymers near the order-disorder transition. Macromolecules 27:6922–6935

48. Khandpur AK, Foerster S, Bates FS, Hamley IW, Ryan AJ, Bras W, Almdal K, Mortensen K (1995) Polyisoprene-polystyrene diblock copolymer phase diagram near the order-disorder transition. Macromolecules 28:8796–8806

49. Han CD, Baek DM, Kim JK, Ogawa T, Sakamoto N, Hashimoto T (1995) Effect of volume fraction on the order-disorder transition in low molecular weight polystyrene-block-polyisoprene copolymers. 1. order-disorder transition temperature determined by rheological measurements. Macromolecules 28:5043–5062

50. Han CD, Kim J, Kim JK (1989) Determination of the order-disorder transition temperature of block copolymers. Macromolecules 22:383–394

51. Han CD, Kim J (1987) Rheological technique for determining the order–disorder transition of block copolymers. J Polym Sci B Polym Phys 25:1741–1764

52. Han CD, Kim JK (1989) Molecular theory for the viscoelasticity of compatible polymer mixtures. 2. Tube model with reptation and constraint release contributions. Macromolecules 22:4292–4302

53. Dae Han C, Kim JK (1993) On the use of time-temperature superposition in multicomponent/multiphase polymer systems. Polymer 34:2533–2539

54. Huggins ML (1961) Viscoelastic Properties of Polymers. J Am Chem Soc 83:4110–4111

55. Hoffman EJ (1972) Viscoelastic Transition. J Eng Ind 94:732–737

56. Faerber GL, Kim SW, Eyring H (1970) Viscous flow and glass transition temperature of some hydrocarbons. J Phys Chem 74:3510–3518

57. Li Y, Liu X, Zhuang X, Jin X, Liu Q (2016) Rheological behavior and spinnability of ethylamine hydroxyethyl chitosan/cellulose co-solution in N-methylmorpholine-N-oxide system. Fibers and Polymers 17:778–788

58. Drabek J, Zatloukal M, Martyn M (2018) Effect of molecular weight on secondary Newtonian plateau at high shear rates for linear isotactic melt blown polypropylenes. J Non-Newtonian Fluid Mech 251:107–118

59. Yanovsky Y (1993) Polymer Rheology: Theory and Practice

60. Zheng Q, Du M, Yang B, Wu G (2001) Relationship between dynamic rheological behavior and phase separation of poly(methyl methacrylate)/poly(styrene-co-acrylonitrile) blends. Polymer 42:5743–5747

61. Zheng Q, Zhang XW, Pan Y, Yi XS (2002) Polystyrene/Sn–Pb alloy blends. I. Dynamic rheological behavior. J Appl Polym Sci 86:3166–3172